Supplementary Material

SiO_2-Templated High-Entropy Spinel Oxides with Abundant Oxygen Vacancies Enabling Lattice-Oxygen-Mediated Oxygen Evolution

Jingyi Zhang [a], Minghui Yu [a], Meiqing Shen [a,c,d], Feng Gao [c,d], Gurong Shen [b,*]

[a] *School of Chemical Engineering and Technology, Tianjin University, Tianjin 300350, PR China*

[b] *School of Materials Science and Engineering, Tianjin University, Tianjin 300350, PR China*

[c] *National Rare Earth Catalysis Research Institute, Dongying 257000, PR China*

[d] *State Key Laboratory of Engines, Tianjin University, Tianjin 300072, PR China*

[*] Corresponding author.

E-mail address: gr_shen@tju.edu.cn

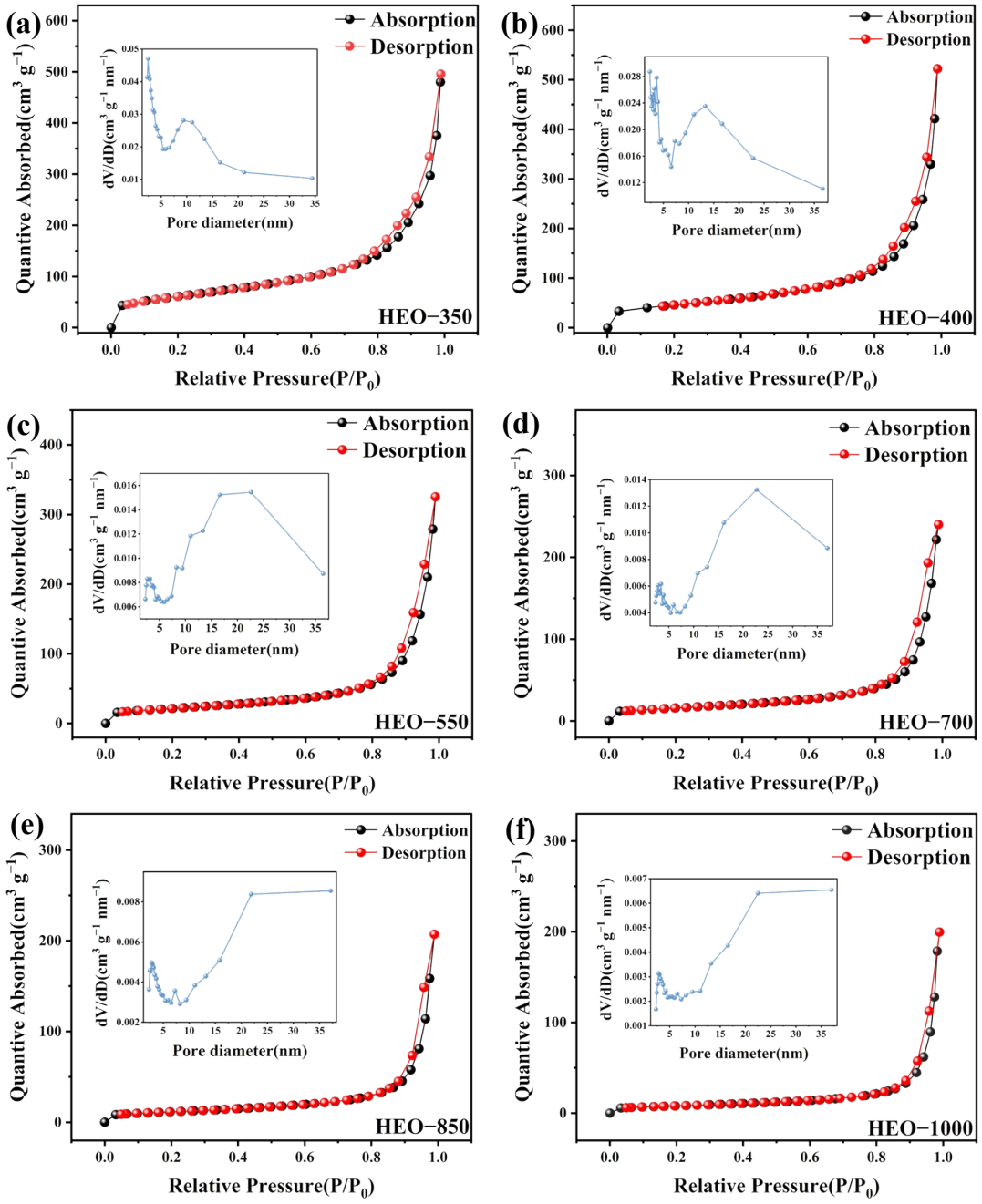

Fig. S1. N_2 absorption/desorption curves and corresponding pore distribution plots of HEO–T catalysts.

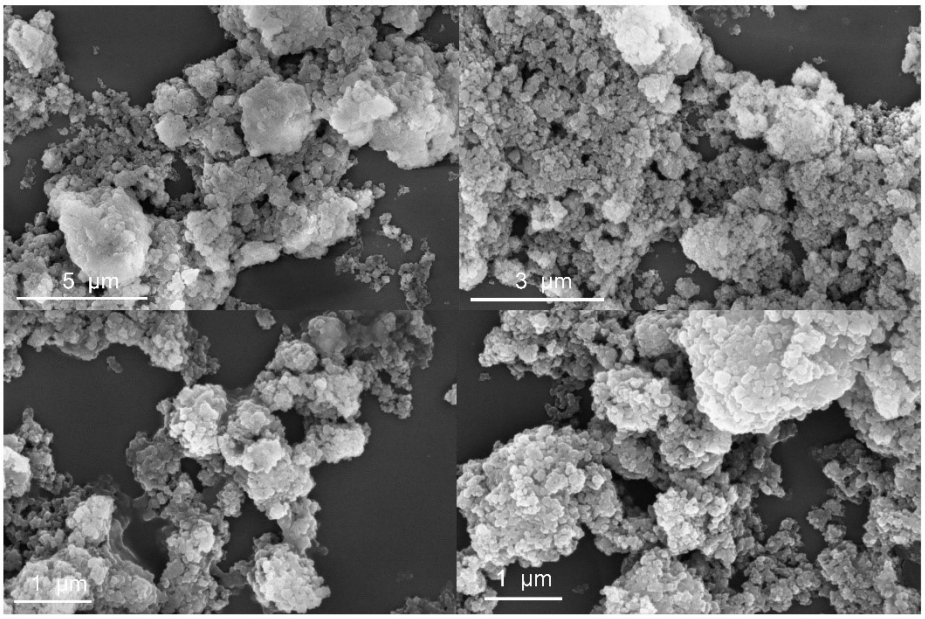

Fig. S2. SEM images of the sample before NaOH etching.

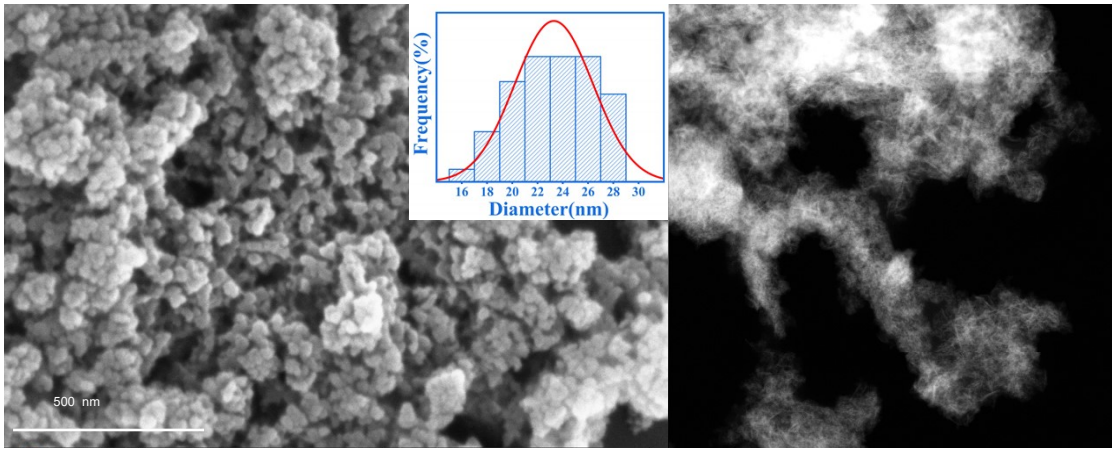

Fig. S3. SEM image with the inset showing the corresponding particle size distribution histogram and HADDF-STEM image of HEO–350.

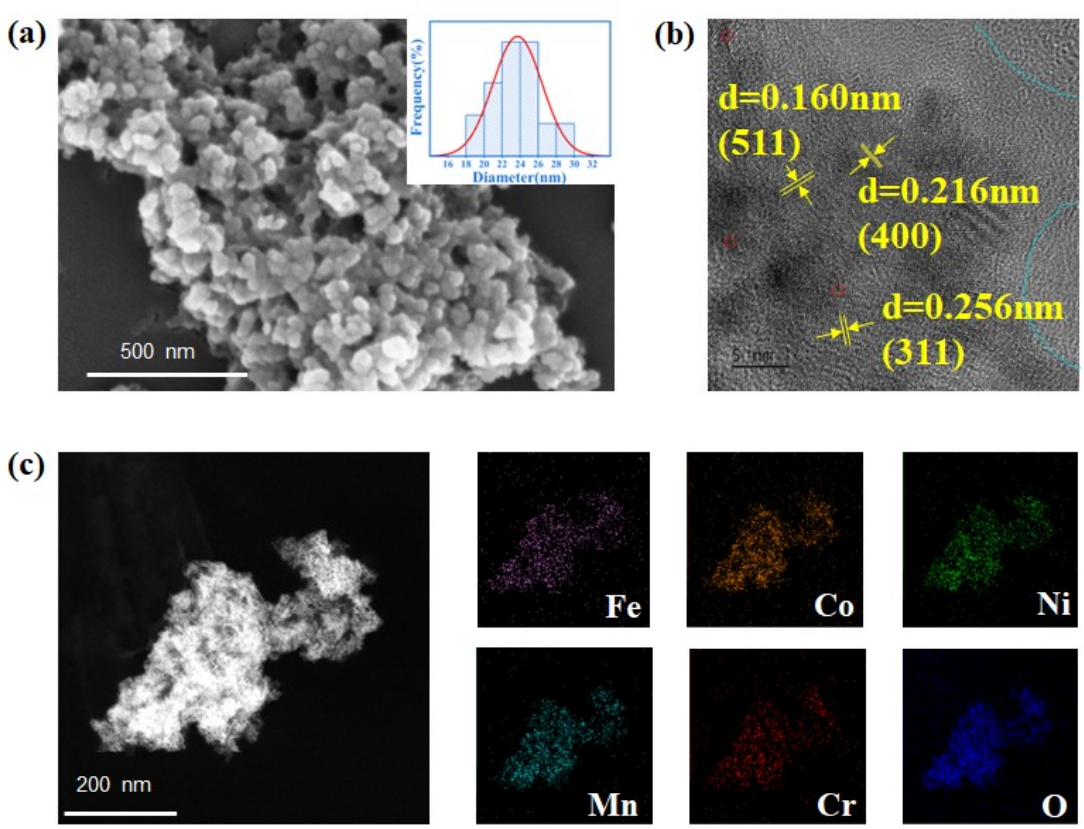

Fig. S4. (a) SEM image, (b) HRTEM image, (c) EDS mapping of HEO–400.

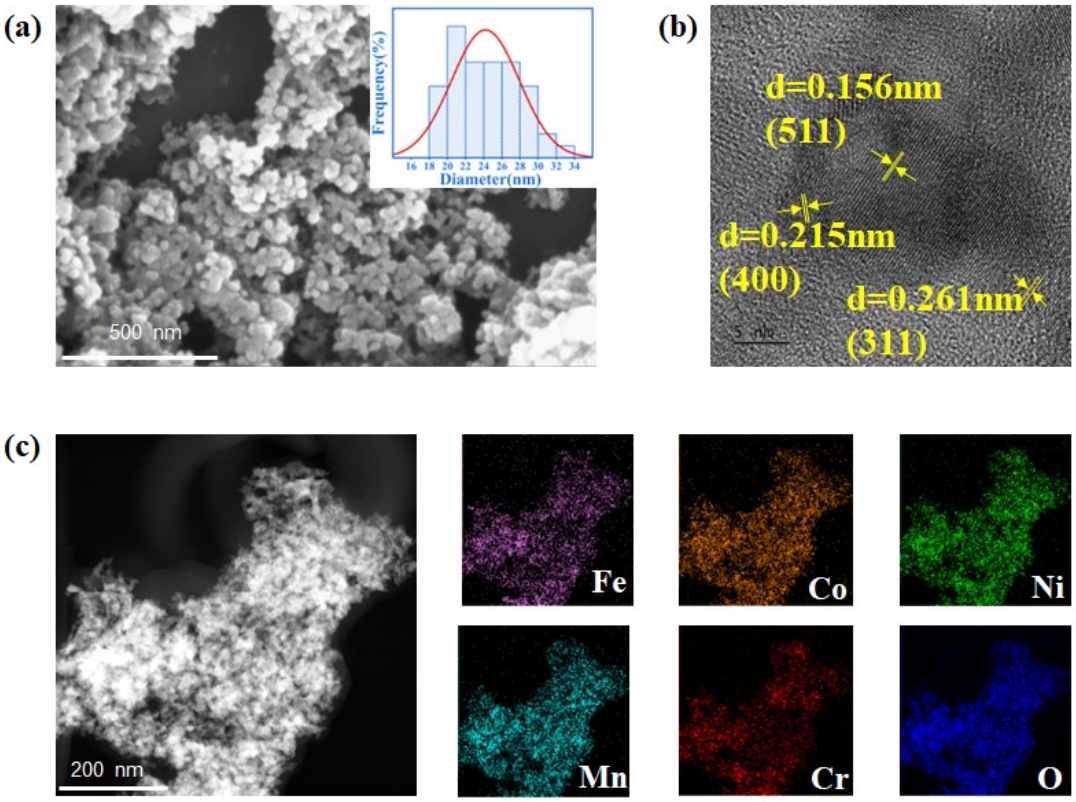

Fig. S5. (a) SEM image, (b) HRTEM image, (c) EDS mapping of HEO–550.

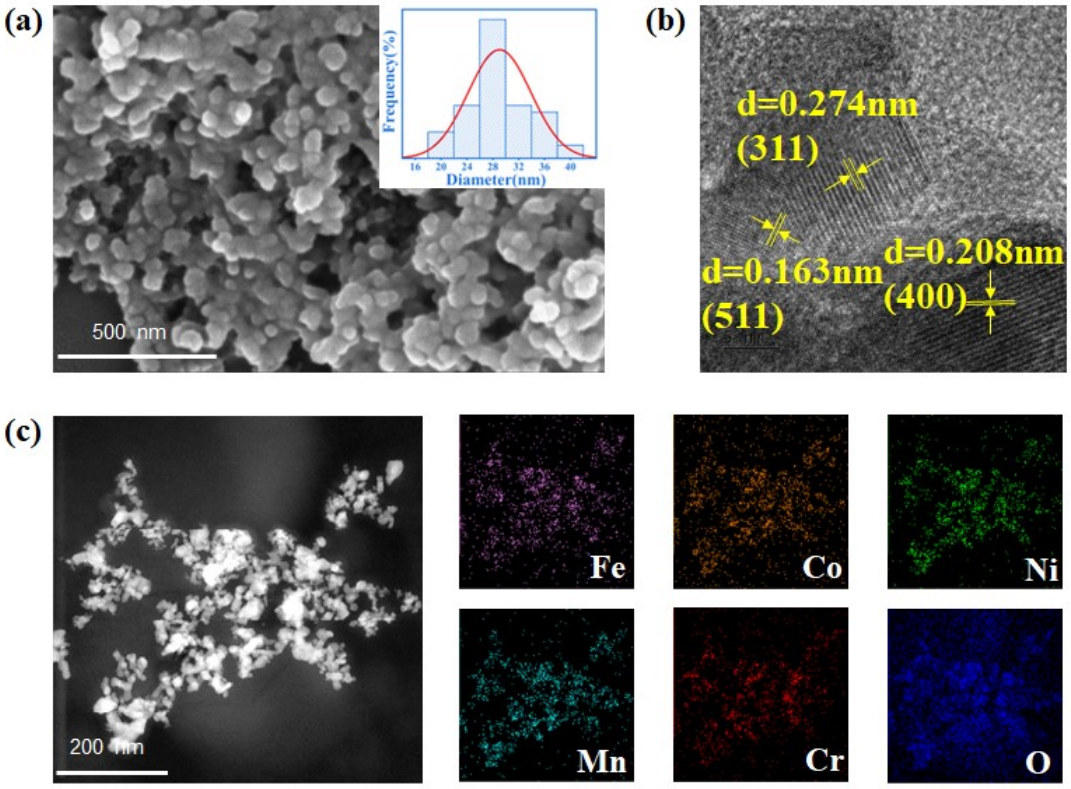

Fig. S6. (a) SEM image, (b) HRTEM image, (c) EDS mapping of HEO–700.

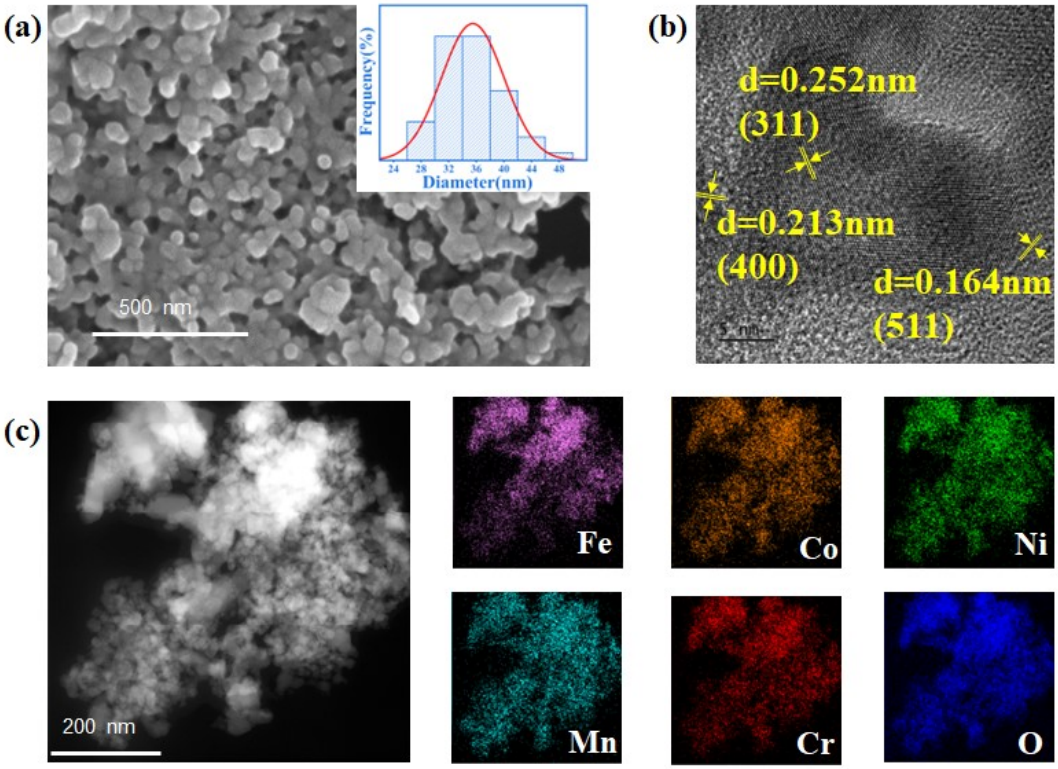

Fig. S7. (a) SEM image, (b) HRTEM image, (c) EDS mapping of HEO–850.

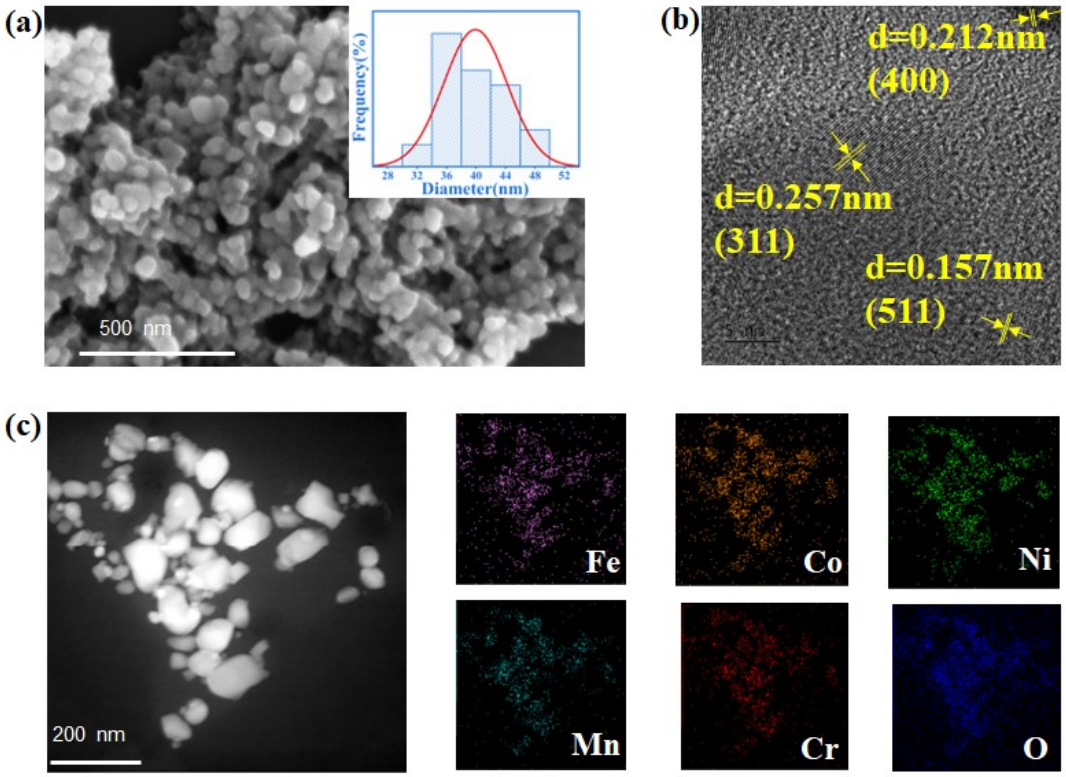

Fig. S8. (a) SEM image, (b) HRTEM image, (c) EDS mapping of HEO–1000.

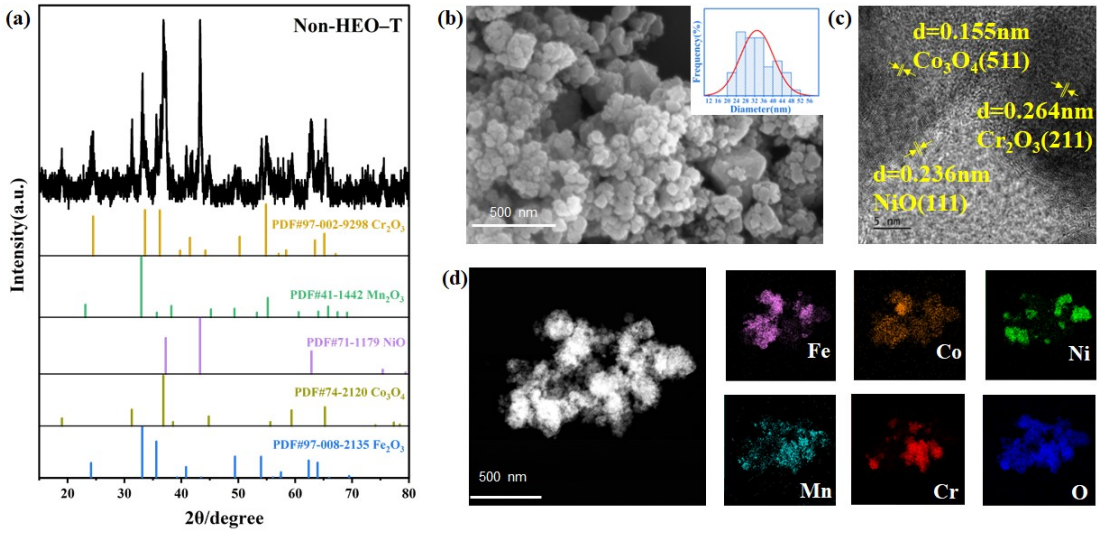

Fig. S9. (a) XRD pattern of Non-HEO–T, (b) SEM image, (c) HRTEM image, (d) EDS mapping of the Non-HEO–T catalyst.

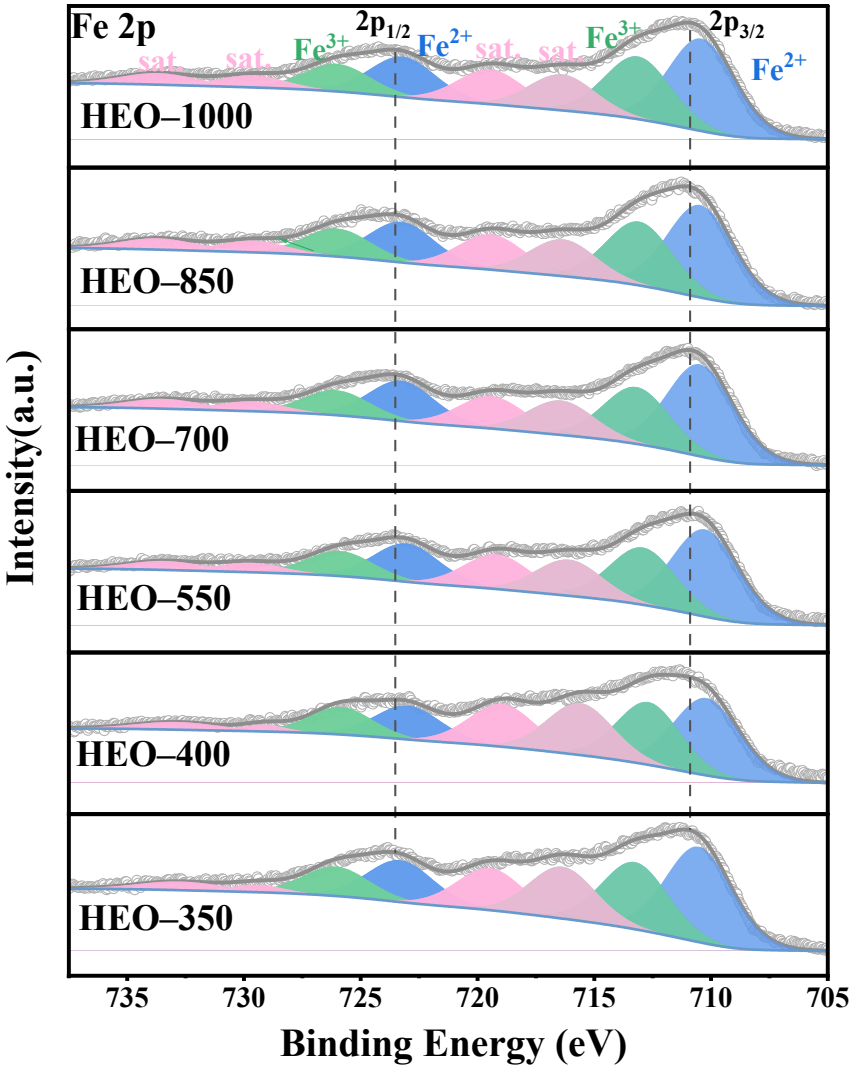

Fig. S10. XPS survey spectrum of Fe 2p of HEO–T catalysts.

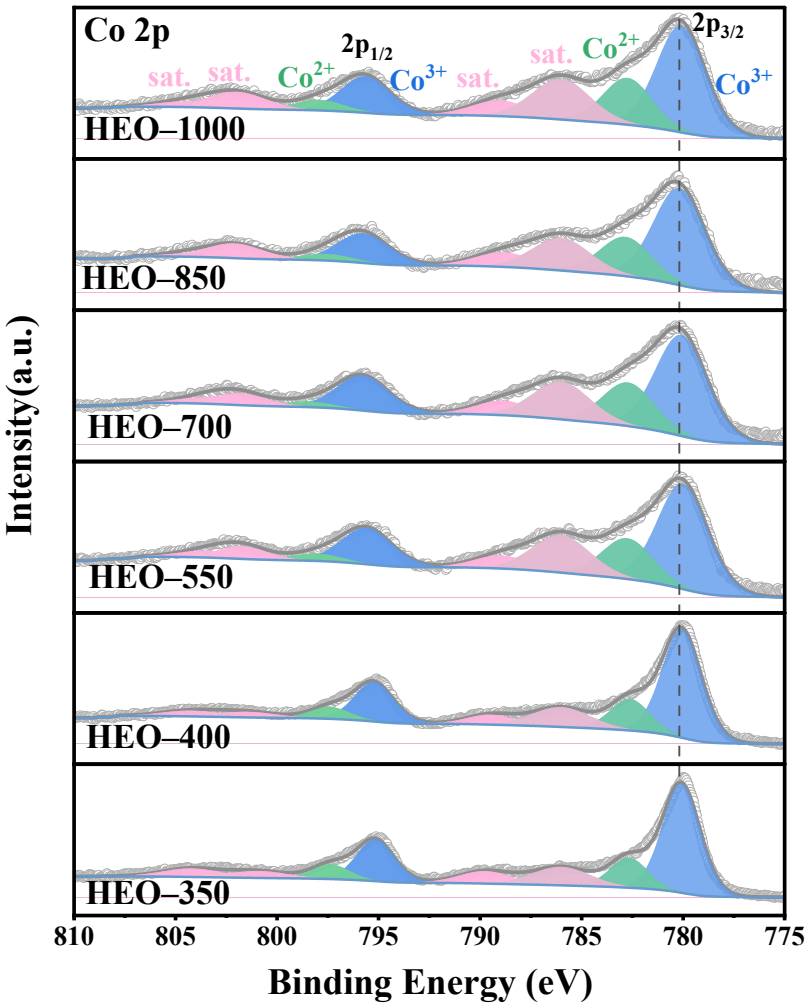

Fig. S11. XPS survey spectrum of Co 2p of HEO–T catalysts.

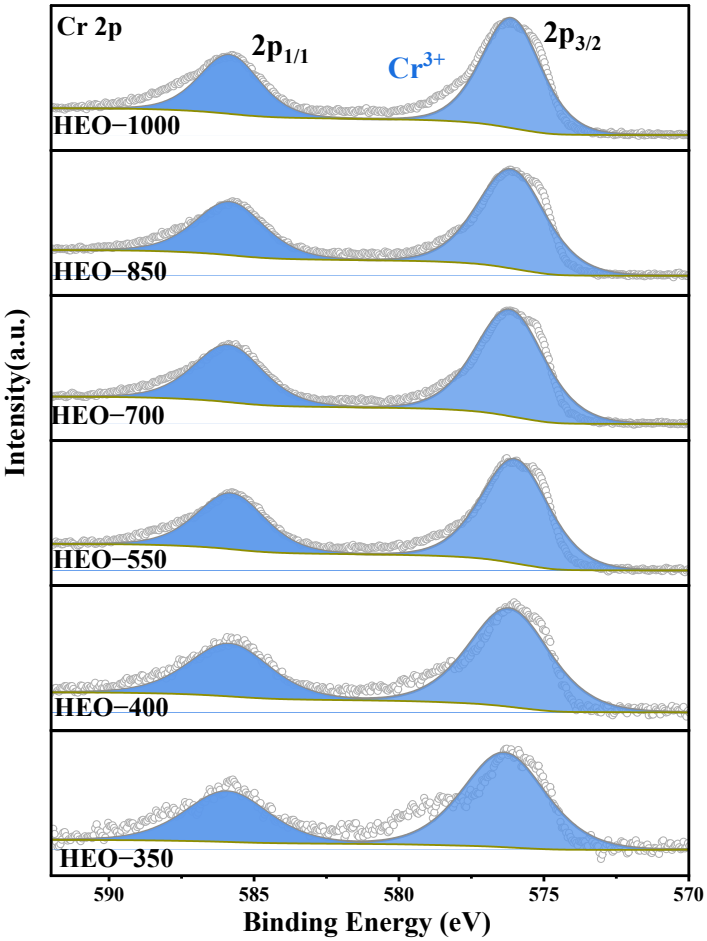

Fig. S12. XPS survey spectrum of Cr 2p of HEO–T catalysts.

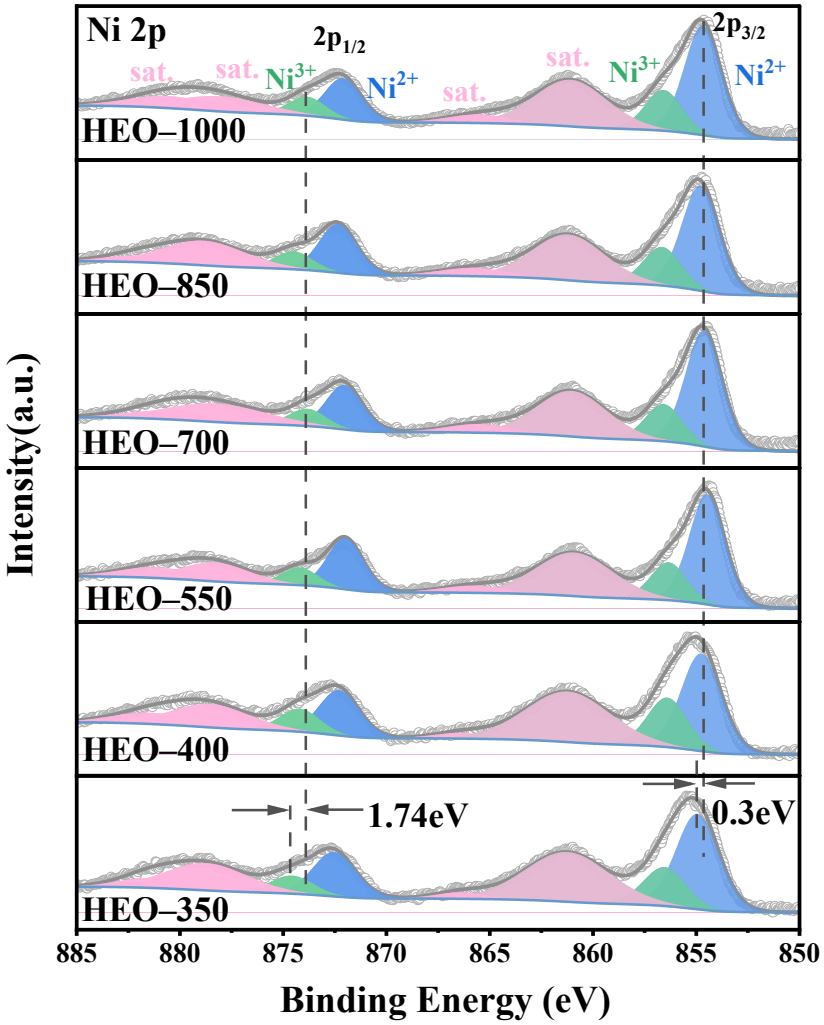

Fig. S13. XPS survey spectrum of Ni 2p of HEO–T catalysts.

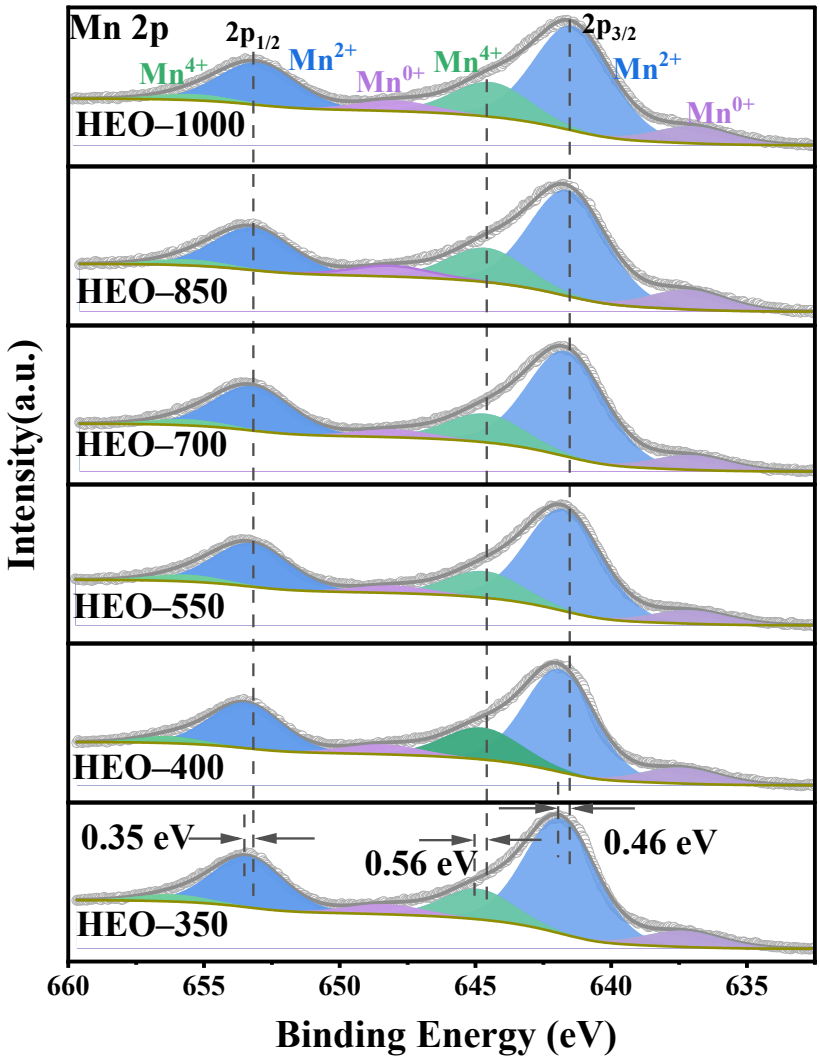

Fig. S14. XPS survey spectrum of Mn 2p of HEO–T catalysts.

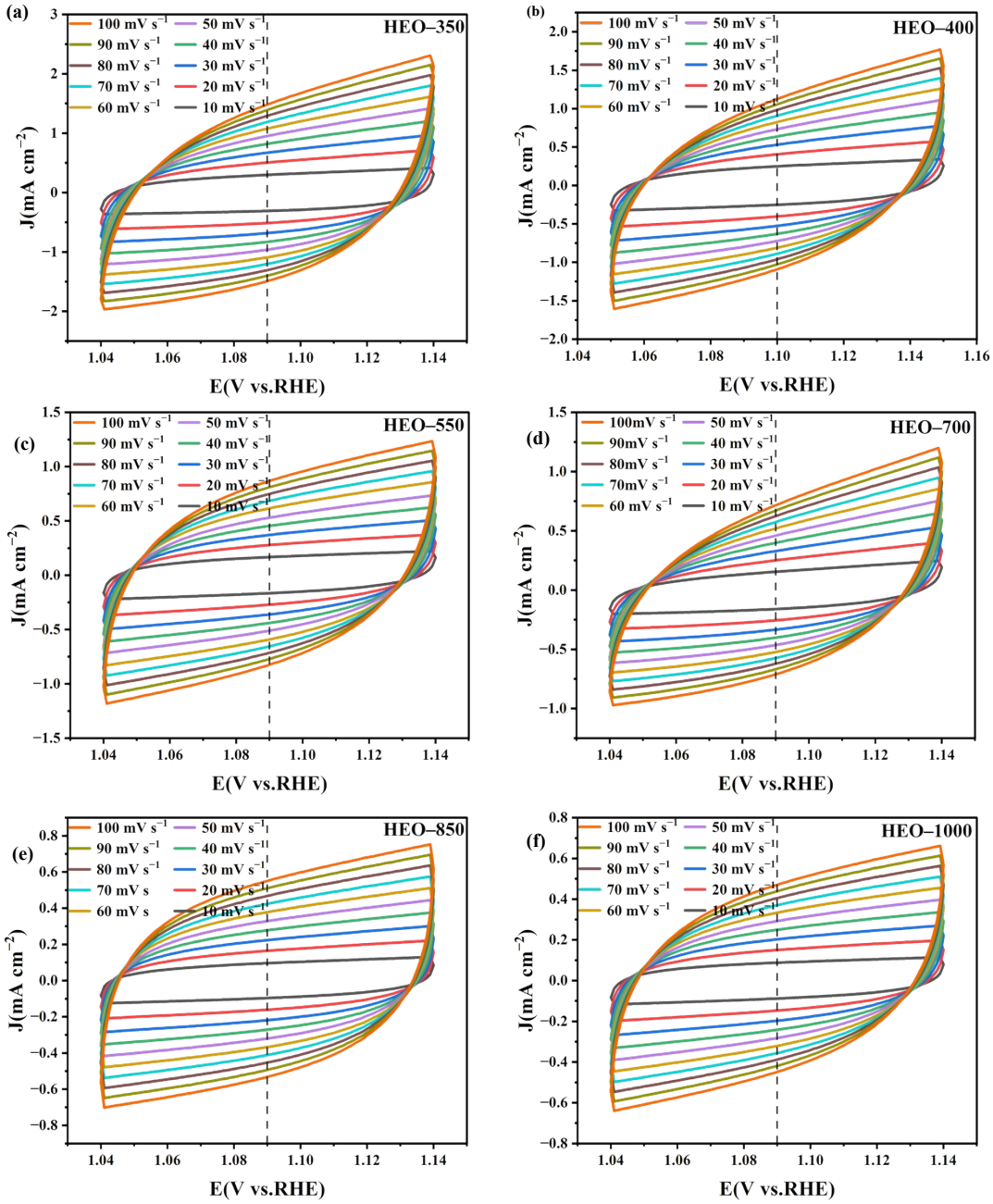

Fig. S15. Cyclic voltammetry measurements of (a) HEO–350, (b) –400, (c) –550, (d) –700, (e) –850, and (f) –1000 in a non-Faradaic potential region at various scan rates.

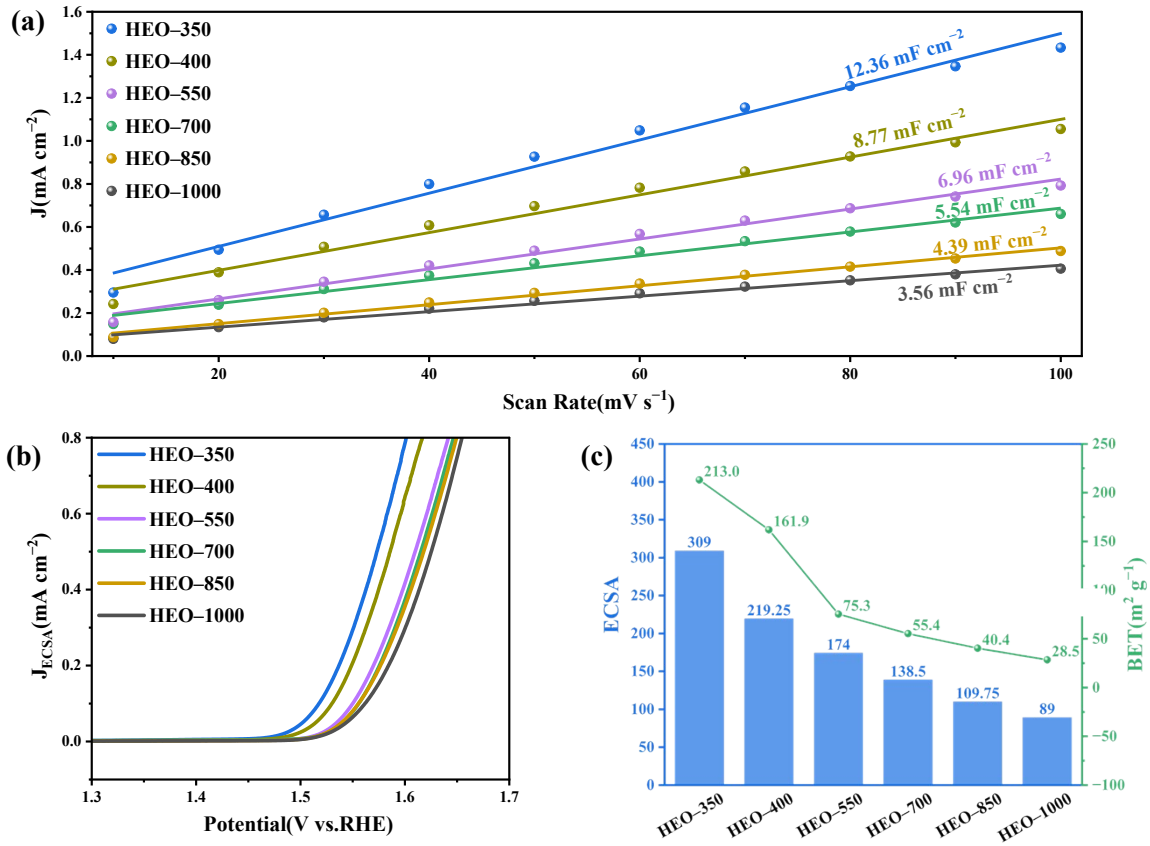

Fig. S16. (a) C_{dl}, (b) Normalized LSV curve of ECSA, (c)ECSA and specific surface area.

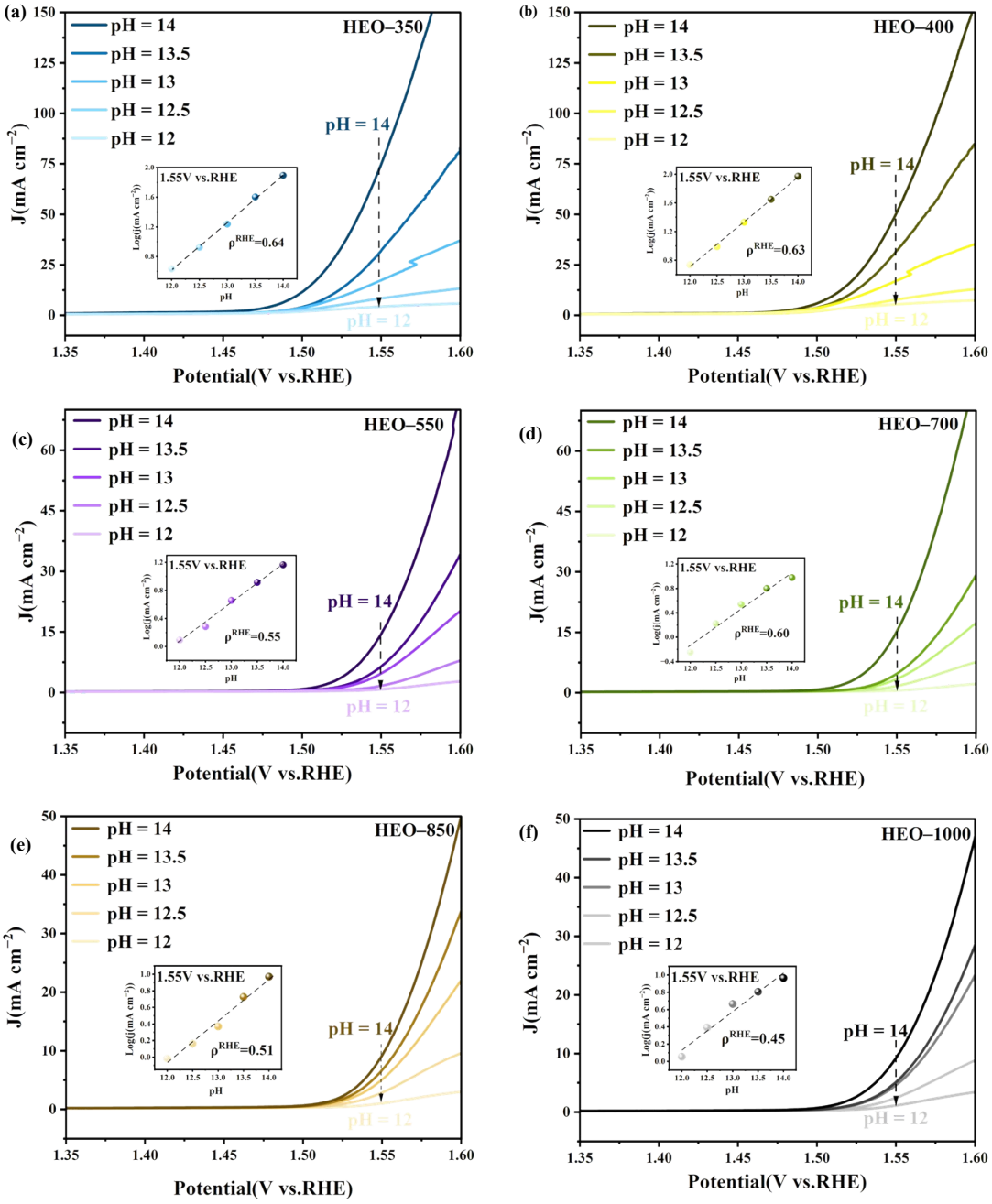

Fig. S17. pH dependence of the OER activities of HEO–T.

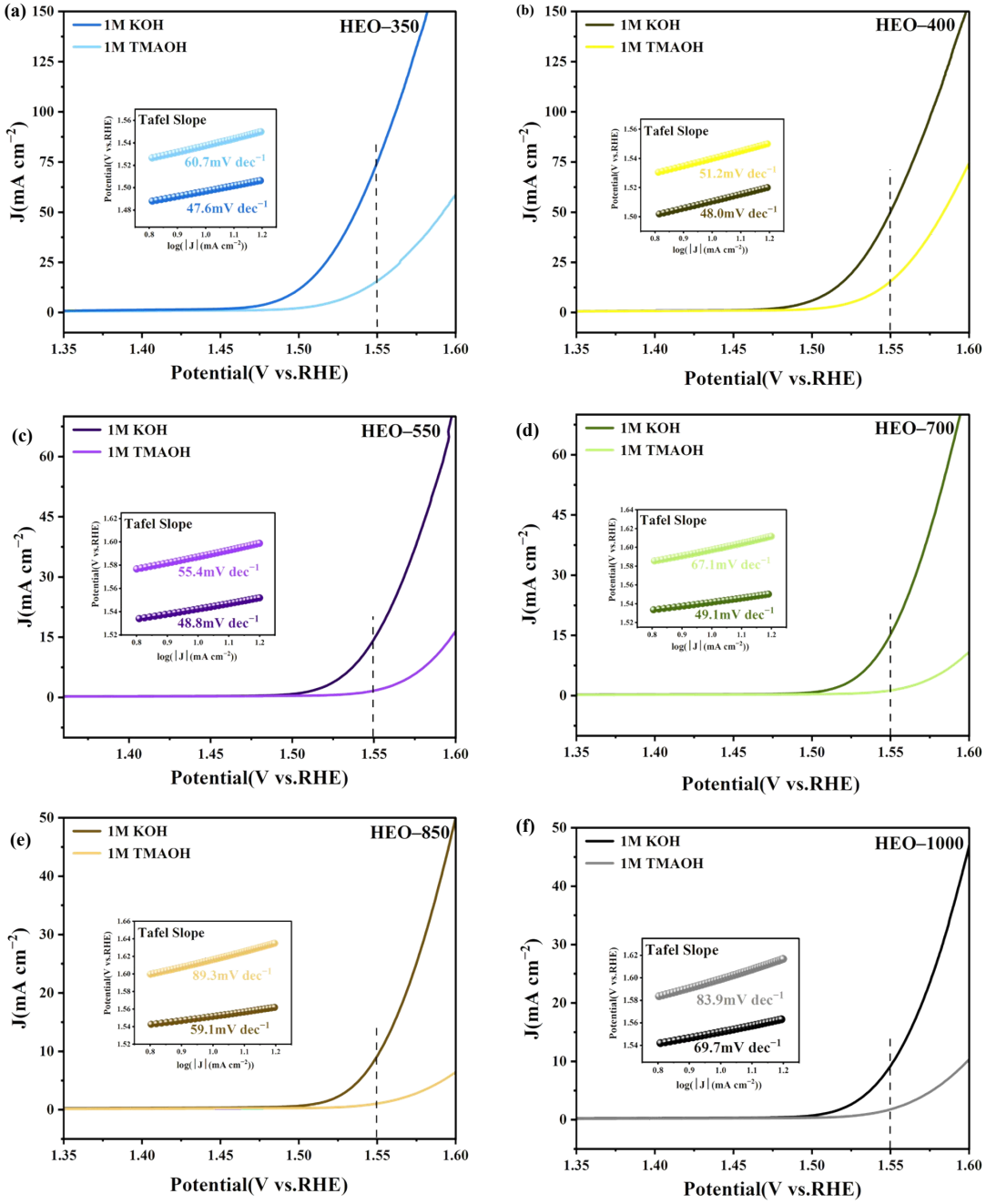

Fig. S18. The polarization curves of HEO–T in 1 M KOH and 1 M TMAOH.

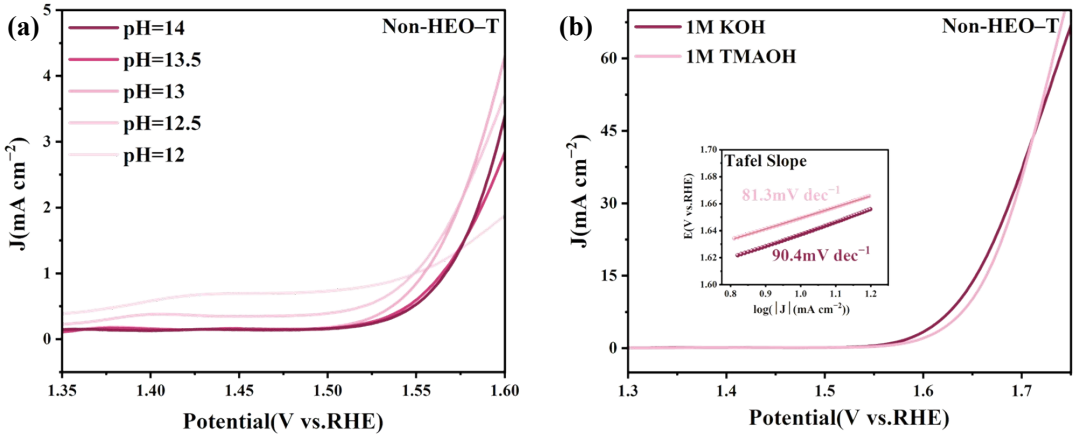

Fig. S19. The polarization curves of Non-HEO–T catalyst (a) in KOH with different pH, (b) in 1 M KOH and TMAOH, respectively.

Table S1. The results of Pore size information of catalyst from BET.

Sample	HEO–350	HEO–400	HEO–550	HEO–700	HEO–850	HEO–1000
Specific Surface Area [$m^2\ g^{-1}$]	213	162	75	55	40	29
Pore Size [nm]	7.20	9.98	13.37	13.41	15.85	21.68
Pore Volume [$cm^3\ g^{-1}$]	0.77	0.80	0.50	0.37	0.32	0.31

Table S2. ICP-OES results of the mole fractions of each metal element before and after NaOH etching.

Steps	Sample	Fe(%)	Co(%)	Ni(%)	Mn(%)	Cr(%)	Total	S_{config}
Before NaOH Etching	HEO−350	21.48	21.94	22.20	21.67	12.71	100.00	1.59R
	HEO−400	18.50	24.76	22.07	20.12	14.55	100.00	1.59R
	HEO−550	20.86	20.37	20.53	19.69	18.55	100.00	1.61R
	HEO−700	20.33	20.69	21.03	18.88	19.07	100.00	1.61R
	HEO−850	20.11	20.42	21.32	19.00	19.15	100.00	1.61R
	HEO−1000	19.12	20.62	20.90	20.12	19.24	100.00	1.61R
After NaOH Etching	HEO−350	22.40	23.70	23.80	22.20	7.90	100.00	1.55R
	HEO−400	15.70	30.80	22.20	20.40	10.90	100.00	1.55R
	HEO−550	20.00	21.30	21.30	19.40	18.00	100.00	1.61R
	HEO−750	19.90	21.10	21.30	18.70	19.00	100.00	1.61R
	HEO−800	19.70	20.80	21.00	18.80	19.70	100.00	1.61R
	HEO−1000	19.50	21.40	21.10	18.70	19.30	100.00	1.61R

Table S3. ICP content of metal ions in the electrolyte after OER reaction

Sample	Fe (ppm)	Co (ppm)	Ni (ppm)	Mn (ppm)	Cr (ppm)
Electrolyte after OER test	0.00	0.00	0.00	0.00	0.00

Table S4. The specific peak positions of Fe 2p, Co 2p and Cr 2p of HEO–T catalysts.

name	Peak BE (eV)	name	Peak BE (eV)
Fe^{2+} $2p_{3/2}$	710.52	Co^{3+} $2p_{3/2}$	780.09
Fe^{2+} $2p_{1/2}$	723.32	Co^{3+} $2p_{1/2}$	795.16
Fe^{3+} $2p_{3/2}$	713.26	Co^{2+} $2p_{3/2}$	782.67
Fe^{3+} $2p_{1/2}$	726.06	Co^{2+} $2p_{1/2}$	797.36
satellite	716.37	satellite	786.00
satellite	719.46	satellite	789.75
satellite	729.42	satellite	800.91
satellite	732.73	satellite	804.23
Cr^{3+} $2p_{3/2}$	576.29	Cr^{3+} $2p_{1/2}$	585.83

Table S5. Elemental composition of HEO−T obtained from XPS.

Sample	Fe (%)	Co (%)	Ni (%)	Mn (%)	Cr (%)	Total
HEO−350	25.45	22.65	20.14	27.82	3.94	100.00
HEO−400	22.80	23.81	19.29	27.85	6.95	100.00
HEO−550	23.26	16.67	17.57	29.69	12.81	100.00
HEO−700	21.83	18.50	17.75	28.66	13.26	100.00
HEO−850	21.78	18.11	21.13	25.75	13.23	100.00
HEO−1000	23.18	17.49	19.01	26.79	13.53	100.00

Table S6. Comparison of the OER activities of HEO–350 with other high entropy catalysts at 10 mA cm^{-2} current density.

Catalyst	Overpotential (mV)	Tafel slope (mV dec^{-1})	Ref.
HEO–350	267	47.6	This work
HEO–400	281	48.0	This work
HEO–550	309	48.8	This work
HEO–700	318	49.1	This work
HEO–850	323	59.1	This work
HEO–1000	335	69.7	This work
Non-HEO–T	407	81.3	This work
$La(Cr_{0.2}Mn_{0.2}Fe_{0.2}Co_{0.2}Ni_{0.2})O_3$	290	54.4	*Adv. Fiber Mater.*, 2025, **7**, 563–573
$ZnCo_2O_4$-xFX/CNTs	350	59.2	*Angew Chem Int Ed*, 2023, **62**, e202301408
$(CoNiMnZnFe)_3O_{3.2}$	336	47.5	*J. Alloys Compd.*, 2021, **868**, 159064
$Sr_{0.95}Co_{0.8}Fe_{0.2}O_{3-\delta}$	370	49.0	*Electrochim. Acta*, 2019, **300**, 85–92
$La_{0.7}Sr_{0.3}Co_{0.2}Mn_{0.2}Ni_{0.2}Fe_{0.2}Al_{0.2}O_{3-x}$	339	73.9	*Int. J. Hydrogen Energy*, 2024, **84**, 192-199
$(Ba_{0.9}La_{0.1})_{0.9}Co_{0.6}Fe_{0.2}Ni_{0.2}O_{3-\delta}$	294	55.0	*Int. J. Hydrogen Energy*, 2024, **51**, 593–604
$Sr_{0.9}Ce_{0.05}Fe_{0.95}Ru_{0.05}O_3$-$RuO_2$	295	77.0	*Nanoscale*, 2023, **15**, 677–686
Co_3O_4/Co-Fe oxide	297	61.0	*Adv. Mater.*, 2018, **30**, 1801211
$La(CrMnFeCoNi)O_3$	325	51.0	*Adv. Fiber Mater.*, 2021, **31**, 2101632
(FeCoNiCuZn)O	323	64.5	*Chem. Eng. J.*, 2024, **481** 148428